Journal of Computational and Applied Mathematics 259 (2014) 937–943

Contents lists available at ScienceDirect

Journal of Computational and Applied Mathematics

journal homepage: www.elsevier.com/locate/cam

Topological flow structures in an L-shaped cavity with horizontal motion of the upper lid

A. Deliceoğlu [a,*], S. Han Aydın [b]

[a] Department of Mathematics, Erciyes University, Kayseri, Turkey

[b] Department of Mathematics, Karadeniz Technical University, Trabzon, Turkey

ARTICLE INFO

Article history:
Received 14 February 2013
Received in revised form 29 August 2013

Keywords:
L-shaped cavity
Flow structure
Bifurcations

ABSTRACT

The flow patterns in a steady, viscous L-shaped cavity are investigated using both analytic solutions combined with methods from nonlinear dynamical systems and numerically using the finite element method. A boundary value problem is formulated for the case of Stokes flow, which is solved analytically, ψ, expressed as an infinite series of eigenfunctions which depend on h_1 and h_2 which are related to the heights of the L-shaped domain. The (h_1, h_2) control space diagram is constructed for exhibiting the mechanism by which new eddies are obtained in the cavity.

© 2013 Elsevier B.V. All rights reserved.

1. Introduction

The main objective of this article is to investigate flow bifurcations in an L-shaped cavity with horizontal motion of the upper lid using ideas from nonlinear dynamical systems (as in [1]) and an analytic solution.

The topic of flow bifurcations in two-dimensional incompressible flow has been one of the interesting research areas in fluid dynamics. These investigations are often related to the qualitative properties of fluid flows in the vicinity of a fixed wall or away from boundaries. Examples include the flow in a rectangular cavity [2–5], the wake flow behind bluff bodies [6] and vortex breakdown [7–9].

The topology and structural stability of flow patterns near a critical point on a stationary wall was studied by Bakker [10]. He used a Taylor series expansion of the velocity vector field near a critical point. Hartnack [11] has also considered bifurcations close to fixed (possibly curved) walls by using normal form transformations. A normal form transformation is a tool for simplifying a stream function to the ones with the simplest order terms. This technique was first used by Brøns and Hartnack [12] for investigating streamline topology near simple degenerate critical points away from boundaries.

There is a wealth of literature on cavity flows which are studied both analytically and numerically (see [13–16]). Gürcan [17] considered the cavity problem to investigate streamline topologies near a non-simple degenerate critical point away from boundaries. Gürcan [18,19] also investigated flow patterns in a single lid-driven cavity using analytic solution for the stream function expanded about any critical point and one of the most important results from these works is an understanding of how the single vortex at small (height to width) aspect ratio A develops into a three vortex pattern as A is increased.

In contrast to flow transformation and eddy generation in a rectangular cavity, there are few studies which examine the genesis of eddies in an L-shaped cavity. Recently, Deliceoğlu and Aydın [1] addressed numerically the problem for the L-shaped cavity with the lids moving in opposite directions. They used a standard Galerkin finite element method for the solution of the Stokes equation and with a stabilization technique for the Navier–Stokes equation. These authors obtained a vortex ring at the reentrant corner and exhibit the mechanism by which new eddies are obtained in the cavity as (h_1, h_2) is varied.

* Corresponding author. Tel.: +90 3524375262; fax: +90 3524374933.
E-mail addresses: adelice@erciyes.edu.tr (A. Deliceoğlu), shaydin@ktu.edu.tr (S.H. Aydın).

0377-0427/$ – see front matter © 2013 Elsevier B.V. All rights reserved.
http://dx.doi.org/10.1016/j.cam.2013.10.007

In the present study, we construct a control-space diagram for the L-shaped cavity by using the analytic solution for the stream function. A control-space diagram exhibits several bifurcation curves representing flow bifurcations at degenerate critical points. This paper is a follow-up of previous study [1] investigating eddy genesis for lids moving in the same directions. Therefore, the same numerical solution procedure is used for the solution of the problem.

2. Governing equation and series solution

We consider the two-dimensional geometry as shown in Fig. 1. Flow in an L-shaped cavity is governed by the incompressible Navier–Stokes equation. It is assumed that the fluid is Newtonian and incompressible with density ρ and viscosity μ. The flow is steady and two dimensional in the (x, y) plane with velocity $\mathbf{u} = (u, v)$. Boundary conditions are specified in terms of velocity components. However, stream function boundary conditions can be derived from velocity boundary conditions in order to obtain the solution for the stream function. In non-dimensional form, the width of the cavity is fixed ($L = 1$), but the heights of the lower side and the upper side, called h_1 and h_2, are varying. Then, the flow behavior is examined by changing the values of both h_1 and h_2.

The steady-state slow, viscous and incompressible fluids, and incompressible Navier–Stokes equations in an open bounded domain $\Omega \subset \Re^2$ with the boundary $\partial\Omega$ are given by

$$\begin{cases} (\nabla \mathbf{u})\mathbf{u} - \dfrac{1}{\mathrm{Re}}\triangle \mathbf{u} + \nabla p = \mathbf{f} & \text{in } \Omega, \\ \nabla \cdot \mathbf{u} = 0 & \text{in } \Omega, \\ \mathbf{u} = 0 & \text{on } \partial\Omega\,. \end{cases} \tag{1}$$

The Stokes equation is the simplified form of the full Navier–Stokes equation (1) for incompressible Newtonian fluid flows for a small Reynolds number. Therefore, the Stokes flow equation is written by ignoring the convective (nonlinear) terms in Eqs. (1) as

$$\begin{aligned} &-\frac{1}{\mathrm{Re}}\triangle \mathbf{u} + \nabla p = \mathbf{f} \quad \text{in } \Omega, \\ &\nabla \cdot \mathbf{u} = 0 \quad \text{in } \Omega. \end{aligned} \tag{2}$$

If we assume that the external force ($\mathbf{f}$) is zero, then the equation is written as a biharmonic operator in terms of stream function, ψ, as

$$\begin{cases} \nabla^4 \psi = \dfrac{\partial^4 \psi}{\partial x^4} + 2\dfrac{\partial^4 \psi}{\partial x^2 \partial y^2} + \dfrac{\partial^4 \psi}{\partial y^4} = 0, \quad \text{in } \Omega, \\ \psi = 0, \qquad \dfrac{\partial \psi}{\partial n} = 0, \quad \text{on } \partial\Omega. \end{cases} \tag{3}$$

The velocity components are expressed in terms of the stream function ψ:

$$u = \frac{\partial \psi}{\partial y}, \qquad v = -\frac{\partial \psi}{\partial x}, \tag{4}$$

where ψ is a solution of the biharmonic equation (3). Using the relations (4), the no-slip conditions for the upper and lower lids and four stationary walls can be written in terms of derivatives of the stream function as

$$\begin{aligned} &\frac{\partial \psi}{\partial y}(x, 2h_2) = 1, \quad (0 \le x \le 1), \qquad \frac{\partial \psi}{\partial y}(x, 2h_1) = 0, \quad \left(\frac{1}{2} \le x \le 1\right), \\ &\frac{\partial \psi}{\partial x}(0, y) = 0, \quad (0 \le y \le 2h_2), \qquad \frac{\partial \psi}{\partial x}\left(\frac{1}{2}, y\right) = 0, \quad (2h_1 \le y \le 0), \\ &\frac{\partial \psi}{\partial x}(1, y) = 0, \quad \text{for } 2h_1 \le y \le 2h_2. \end{aligned} \tag{5}$$

Therefore, the problem is reduced to the boundary value problem as shown in Fig. 1. This boundary value problem can be solved numerically many different ways. In our study, we consider the standard Galerkin finite element method for the corresponding biharmonic differential equation (Eq. (3)) with the boundary conditions in terms of the unknown function ψ (Eq. (5)) using bilinear quadratic elements (for the details of the numerical method and solution procedure, see [1]).

For the analytical solution; following the process performed by Driesen et al. [20] and Trogdon and Joseph [21], the flow domain is divided into three subregions. For each subregion the resulting series of eigenfunctions is given below.

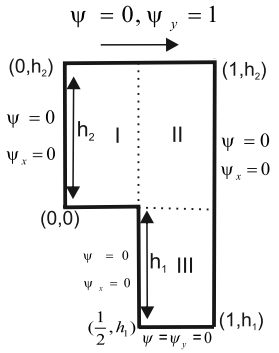

Fig. 1. The boundary value problem for the L-shaped cavity.

The stream function for the first region can be written as

$$\begin{aligned}\psi_1(x,y) = &\sum_{n=-\infty}^{\infty} \frac{\phi_{a,n}(x)}{{\lambda_{a,n}}^2}\left(A_n\frac{\sinh\left(\lambda_{a,n}(y-h_2)\right)}{\sinh(\lambda_{a,n}h_2)} + B_n\frac{\cosh(\lambda_{a,n}(y-h_2))}{\cosh(\lambda_{a,n}h_2)}\right)\\ &+\sum_{n=-\infty}^{\infty} \frac{\phi_{s,n}(x)}{{\lambda_{s,n}}^2}\left(C_n\frac{\sinh\left(\lambda_{s,n}\,(y-h_2)\right)}{\sinh(\lambda_{s,n}h_2)} + D_n\frac{\cosh\left(\lambda_{s,n}(y-h_2)\right)}{\cosh(\lambda_{s,n}h_2)}\right)\\ &+\sum_{n=-\infty}^{\infty} \frac{\xi_{a,n}(y)}{{\mu_{a,n}}^2}\left(E_n\frac{\sinh\left(\mu_{a,n}\left(x-\frac{1}{4}\right)\right)}{\sinh(\mu_{a,n})} + F_n\frac{\cosh\left(\mu_{a,n}\left(x-\frac{1}{4}\right)\right)}{\cosh(\mu_{a,n})}\right)\\ &+\sum_{n=-\infty}^{\infty} \frac{\xi_{s,n}(y)}{{\mu_{s,n}}^2}\left(G_n\frac{\sinh\left(\mu_{s,n}\left(x-\frac{1}{4}\right)\right)}{\sinh(\mu_{s,n})} + H_n\frac{\cosh\left(\mu_{s,n}\left(x-\frac{1}{4}\right)\right)}{\cosh(\mu_{s,n})}\right)\end{aligned}$$

where the functions

$$\phi_{a,n}(x) = s_{a,n}[\sin(s_{a,n})\cos(s_{a,n}(4x-1)) - (4x-1)\cos(s_{a,n})\sin(s_{a,n}(4x-1))], \tag{6}$$

$$\phi_{s,n}(x) = s_{s,n}[\cos(s_{s,n})\sin(s_{s,n}(4x-1)) - (4x-1)\sin(s_{s,n})\cos(s_{s,n}(4x-1))], \tag{7}$$

$$\xi_{a,n}(y) = s_{a,n}\left[\sin(s_{a,n})\cos\left(\frac{s_{a,n}\,(y-h_2)}{h_2}\right) - \left(\frac{y-h_2}{h_2}\right)\cos(s_{a,n})\sin\left(\frac{s_{a,n}\,(y-h_2)}{h_2}\right)\right], \tag{8}$$

$$\xi_{s,n}(y) = s_{s,n}\left[\cos(s_{s,n})\sin\left(\frac{s_{s,n}\,(y-h_2)}{h_2}\right) - \left(\frac{y-h_2}{h_2}\right)\sin(s_{s,n})\cos\left(\frac{s_{s,n}\,(y-h_2)}{h_2}\right)\right] \tag{9}$$

are the symmetric and antisymmetric Papkovich–Fadle eigenfunctions [22,23]. The sidewall boundary conditions (5) are applied to the eigenfunctions which are defined above, one finds that the parameters $s_{a,n}$ and $s_{s,n}$ have to satisfy the eigenvalue equations

$$\sin(2s_{a,n}) = -2s_{a,n}, \qquad \sin(2s_{s,n}) = 2s_{s,n} \tag{10}$$

respectively. The $s_{a,n}$ and $s_{s,n}$ are determined by the Newton iteration procedure described by Robbins and Smith [24] using an initial estimate of the form

$$2s_{a,n} = (2n-1.5)\pi + i\ln(4n-1)\pi - \left[\frac{2\ln(4n-1)\pi}{(4n-1)\pi} + i\frac{4\ln(4n-1)\pi+1}{(4n-1)^2\pi^2}\right] + \cdots, \tag{11}$$

$$2s_{s,n} = (2n+1.5)\pi + i\ln(4n+1)\pi - \left[\frac{2\ln(4n+1)\pi}{(4n+1)\pi} + i\frac{4\ln(4n+1)\pi+1}{(4n+1)^2\pi^2}\right] + \cdots \tag{12}$$

and

$$\lambda_{a,n} = 4s_{a,n}, \qquad \lambda_{s,n} = 4s_{s,n}, \qquad \mu_{a,n} = \frac{\lambda_{a,n}}{h_2}, \qquad \mu_{s,n} = \frac{\lambda_{s,n}}{h_2}. \tag{13}$$

In the same way, the stream functions for the region II and III can also be derived.

3. The formation of eddy structures in an L-shaped cavity

In this section we describe how eddies are generated within the L-shaped cavity as the heights of the lower side (h_1) and upper side (h_2) (see Fig. 1) are varied for $S = 0$ at which the upper lid moves in the horizontal direction. In discussing the formation of eddies, bifurcation curves are obtained to analyze structural bifurcation of the flow caused by varying (h_1, h_2)

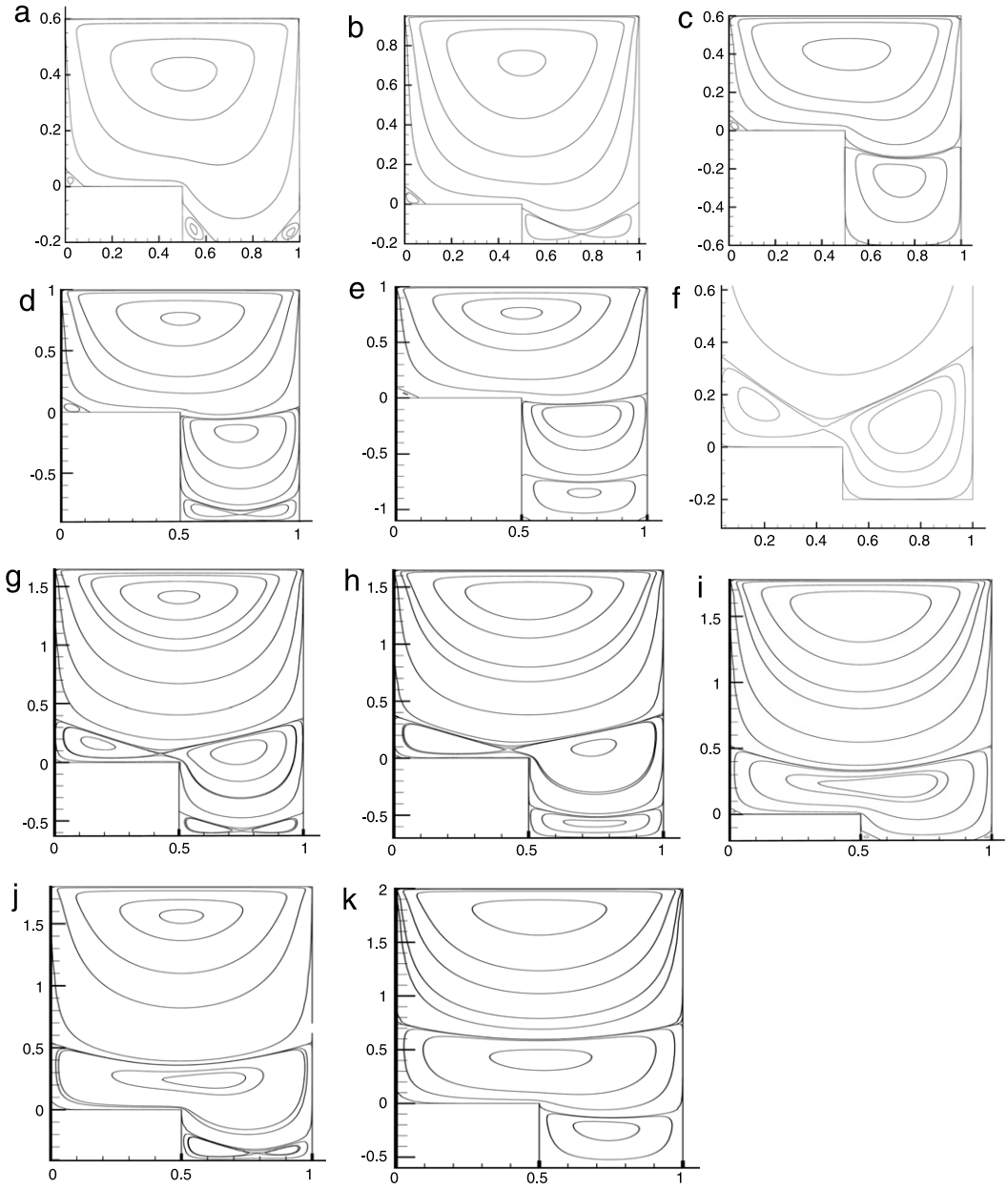

Fig. 2. Representations of the observed flow topologies (contours of the stream function) found in the steady domain. (a) $h_1 = -0.2, h_2 = 0.6$; (b) $h_1 = -0.2, h_2 = 0.95$; (c) $h_1 = -0.6, h_2 = 0.6$; (d) $h_1 = -0.2, h_2 = 1.65$; (e) $h_1 = -0.9, h_2 = 1.0$; (f) $h_1 = -1.1, h_2 = 1.0$; (g) $h_1 = -0.63, h_2 = 1.65$; (h) $h_1 = -0.7, h_2 = 1.65$; (i) $h_1 = -0.2, h_2 = 1.78$; (j) $h_1 = -0.41, h_2 = 1.8$; (k) $h_1 = -0.6, h_2 = 2.0$.

parameters. There are critical values of h_1 and h_2 at which flow bifurcations occur. Namely, at these critical values of h_1 and h_2, the type of stagnation points changes. At stagnation points velocity components (u, v) is zero and so such points are solutions of the equation

$$\dot{x} = u = \frac{\partial \psi}{\partial y} = 0, \qquad \dot{y} = v = -\frac{\partial \psi}{\partial x} = 0. \tag{14}$$

When h_1 and h_2 are varied in the range $-1.4 < h_1 < 0$ and $0.1 < h_2 < 3.2$, we have encountered the 11 distinct flow topologies which are shown in Fig. 2.

Using both the analytical and numerical methods mentioned in Section 2, we have obtained a set of codimension-one bifurcation curves in the (h_1, h_2) parameter space. The codimension of a bifurcation is the smallest number of parameters needed to describe the bifurcation. All figures presented in this study can be tracked either by fixing h_1 and varying h_2 or by fixing h_2 and varying h_1. The corresponding bifurcation curves can then be illustrated in Fig. 3.

3.1. Bifurcation of critical points near a stationary wall

There are two types of degenerate critical points (simple and non-simple) which depend on the Jacobian matrix of the velocity field. The first case, concerning simple degenerate critical points (i.e. a singular non-zero Jacobian matrix), was already examined by Hartnack [11]. He used normal form transformations via a generating function. We briefly show how to simplify fourth order terms of the stream function

$$\psi = y^2 \sum_{i,j=0}^{\infty} a_{i,j+2} x^i y^j. \tag{15}$$

If $a_{0,2} = a_{1,2} = 0$ in (15), the origin is a simple degenerate critical point. To analyze the possible flow patterns close to simple degeneracy, the small parameters $a_{0,2} = \epsilon_1$, $a_{1,2} = \epsilon_2$ are introduced. The new coordinates (ξ, η) are found from a canonical transformation defined by the generating function

$$G = y\xi + \frac{a_{1,3}}{6a_{0,3}} y\xi^2 - \frac{a_{2,2}}{9a_{0,3}} y^2\xi + \frac{2a_{2,2}}{27a_{0,3}^2} y\xi\epsilon \tag{16}$$

such that

$$x = \frac{\partial G}{\partial y}, \qquad \eta = \frac{\partial G}{\partial \xi}. \tag{17}$$

Solving Eq. (17) with respect to x and y and inserting this transformation in (15), the normal form of the stream function is obtained. The method for finding the normal form of bifurcation of critical point proceeds as in the previous study [11]. We omit computation steps and only give the following transformed stream function:

$$\psi = \eta^2 \left(\sigma\eta + b + \frac{1}{2}\xi^2 \right) \tag{18}$$

where

$$b = -\frac{{\epsilon_2}^2}{4a_{0,3}a_{2,2}} - \frac{{a_{1,3}}^2{\epsilon_1}^2}{9a_{2,2}{a_{0,3}}^3} + \frac{\epsilon_1}{a_{0,3}} - \frac{4}{27}\frac{a_{2,2}{\epsilon_1}^2}{{a_{0,3}}^3} + \frac{\epsilon_2 a_{1,3}\epsilon_1}{3a_{2,2}{a_{0,3}}^2}. \tag{19}$$

Hartnack [11] derived the following theorem for the stream function of codimension one.

Theorem 1. *Let ψ be expanded in a power series,*

$$\psi = y^2 \sum_{i,j=0}^{\infty} a_{i,j+2} x^i y^j. \tag{20}$$

Assuming the non-degeneracy conditions $a_{0,3} \neq 0$, $a_{2,2} \neq 0$ a normal form of order 4 for the stream function is,

$$\psi = y^2 \left(\sigma y + b + \frac{1}{2}x^2 \right) \tag{21}$$

where

$$\sigma = \begin{cases} 1 & \text{for } \dfrac{a_{2,2}}{a_{0,3}} > 0 \\ -1 & \text{for } \dfrac{a_{2,2}}{a_{0,3}} < 0 \end{cases}$$

and b is a transformed small parameter.

The bifurcation structure of (21) is shown in Fig. 4(a) and (b). The relevant computation can be found in [8,9,11,10].

Near a stationary wall there are two possible degenerate critical points which are illustrated in Fig. 4(a) and (b). In the first case, a degenerate critical point is created on the stationary wall (Fig. 4(a)), and the critical point bifurcates into a center away from boundaries and two on-wall saddles. In the second case, a bifurcation occurs on the wall at which two on-wall saddle points coalesce to produce an off-wall saddle point, Fig. 4(b). This type of bifurcation is illustrated with BM $(i = 1, \ldots, 5)$ in Fig. 3. Apart from these degenerate points on the wall, there is also an off-wall degenerate point which bifurcates into a saddle and a center, Fig. 4(c). A cusp bifurcation curve is denoted by CP $(i = 1, \ldots, 5)$.

In Fig. 2, we display a series of flow structures for different values of the heights of the lower side (h_1) and upper side (h_2) of the L-shaped cavity. A topology of type (a) has a large vortex and two corner eddies. By varying the (h_1, h_2) parameter space, the corner eddies meet each other along the bubble merging curve BM_1. Then we see that now a region (b) consisting of a large vortex with an inner separatrix. Entering region (c) from (b), the cusp bifurcation curve CP_1 is passed on which the separatrix has disappeared. Hence the genesis of second eddy in the lower part of the cavity is complete as shown in Fig. 2(c). This flow transformation is similar to that observed by Gürcan [18] for the $S = 0$ case.

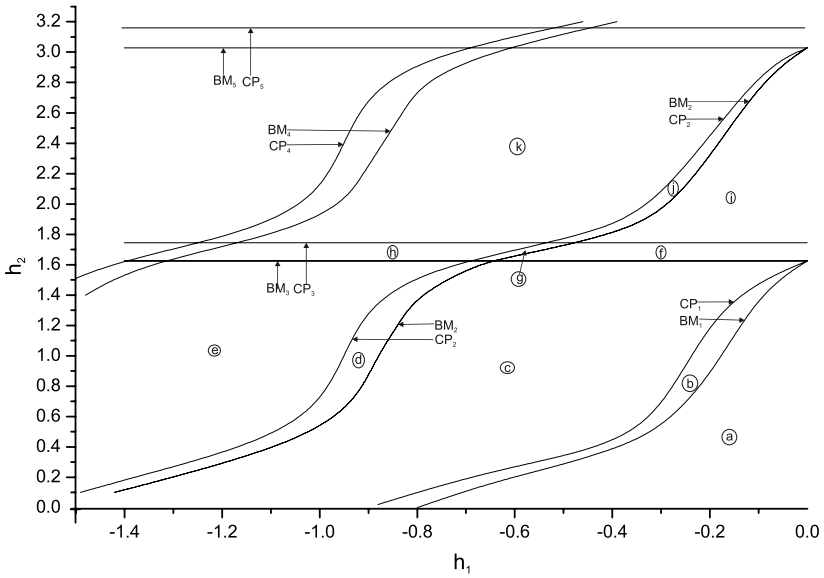

Fig. 3. Control-space diagram for an L-shaped cavity. h_1–h_2 parameter space is split into a number of distinct regions by the bifurcation curves (BM_1, BM_2, BM_3, BM_4, BM_5, CP_1, CP_2, CP_3, CP_4, CP_5). The labels in each region correspond to the flow patterns in Fig. 2.

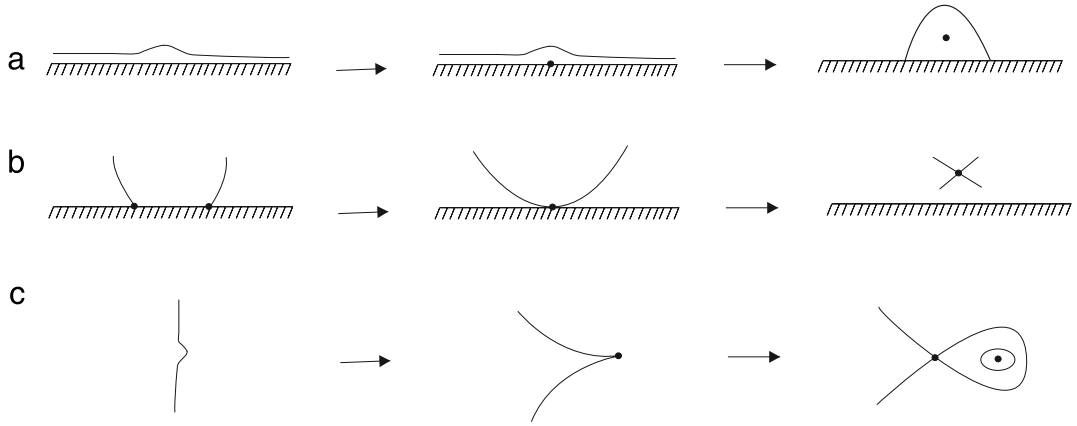

Fig. 4. Local behavior of degenerate critical points close to a stationary wall (a) and (b) and away from boundaries (c).

A dividing streamline which is placed under the reentrant corner moves to the reentrant corner when h_2 is increased in regions (c)–(e). When the bubble merging curve BM_3 reaches a value of 1.625, the dividing streamline separates the upper and lower cavities from the reentrant corner. Apart from the case of the lids moving in opposite directions, which has been studied by Deliceoğlu and Aydın [1], the dividing streamline does not move upstream along the horizontal wall. As h_2 increases it is observed that the corner eddies of the upper cavities grow in size and meet the dividing streamline at the reentrant corner. When (h_1, h_2) crosses the curve BM_3 in the $(c \to f)$, $(d \to g)$ and $(e \to h)$ direction in the control space diagram, a new eddy is obtained with a separatrix. As h_2 is increased beyond the cusp bifurcation curve CP_3, in the middle eddy a separatrix has been replaced by a single eddy (see Fig. 2(k)).

It is observed that two basic bifurcation scenarios occur in the L-shaped cavity with horizontal motion of the upper lid. The first type of bifurcation scenarios can occur on the bottom of the lower cavities. A new eddy is obtained by decreasing the height of the lower cavities, as shown in Fig. 3 $(a \to b \to c)$. The number of eddies increases from one to two. When h_1 is further decreased, Fig. 3 $(c \to d \to e)$ shows that the same bifurcation sequence of flow pattern changes appear in the lower eddy with upper eddies remain unaffected. We have now three eddies in the L-shaped cavity.

The second type of scenarios corresponding to the horizontal band between MB_3 and CP_3 can be seen in Fig. 3. As h_2 increases it can be seen that the lower eddy in region (c) is displaced towards the upper lid in region (i). Possible flow pattern sequences which can occur near the horizontal band between MB_3 and CP_3 are shown in Fig. 3 $(c \to f \to i, d \to g \to j$ and $e \to h \to k)$. The flow patterns labeled in the horizontal band between MB_3 and CP_3 are quite similar to those in the horizontal band between MB_5 and CP_5. For this reason, the relevant parameter range is outside the scope of the present paper.

4. Conclusion

In this paper, we have presented the flow patterns and the genesis of eddies in an L-shaped cavity, where the motion is created by the horizontal motion of the upper lid. The control-space diagram (Fig. 3) demonstrates the effect of the reentrant corner on the behavior of the flow in the L-shaped cavity. It is observed that the corner eddies of the upper part of the cavity meet the separation line at the reentrant corner. It is interesting to notice that the bifurcation curve BM_3 remains at almost the same value (1.62) for the L-shaped and rectangular cavities. Hence the reentrant corner does not affect the location of the saddle–node bifurcation of the upper part of the cavities. Transition patterns in an L-shaped cavity were investigated for $-1.4 < h_1 < 0$ and $0.1 < h_2 < 3.2$. It was also shown that the single eddy structure develops into a three eddy structure via several flow transformations.

References

[1] A. Deliceoğlu, S.H. Aydın, Flow bifurcation and eddy genesis in an L-shaped cavity, Comput. Fluids 73 (2013) 24–46.
[2] F. Gürcan, A. Deliceoğlu, P.G. Bakker, Streamline topologies near non-simple degenerate point close to a stationary wall using normal forms, J. Fluid Mech. 539 (2005) 299–311.
[3] F. Gürcan, A. Deliceoğlu, Streamline topologies near non-simple degenerate points in two-dimensinonal flows with double symmetry away from boundaries and an application, Phys. Fluids 17 (2005) 093106-1–093106-7.
[4] F. Gürcan, A. Deliceoğlu, Saddle connections near degenerate critical points in Stokes flow within cavities, Appl. Math. Comput. 172 (2006) 1133–1144.
[5] A. Deliceoğlu, F. Gürcan, Streamline topologies near non-simple degenerate critical points in two-dimensional flow with symmetry about an axis, J. Fluid Mech. 606 (2008) 417–432.
[6] A.E. Perry, M.S. Chong, T.T. Lim, The vortex-shedding process behind two-dimensional bluff bodies, J. Fluid Mech. 116 (1982) 77–87.
[7] M. Brøns, L.K. Voigt, J.N. Sørensen, Streamline topology of steady axisymmetric vortex breakdown in a cylinder with co-and counter-rotating end-covers, J. Fluid Mech. 401 (1999) 275–292.
[8] M. Brøns, L.K. Voigt, J.N. Sørensen, Topology of vortex breakdown bubbles in a cylinder with a rotating bottom and a free surface, J. Fluid Mech. 428 (2001) 133–148.
[9] M. Brøns, A.V. Bisgaard, Bifurcation of vortex breakdown patterns in a circular cylinder with two rotating covers, J. Fluid Mech. 568 (2006) 329–349.
[10] P.G. Bakker, Bifurcation in Flow Patterns, Klüver Academic, 1991.
[11] J.N. Hartnack, Streamlines topologies near a fixed wall using normal form, Acta Mech. 136 (1999) 55–75.
[12] M. Brøns, J.N. Hartnack, Streamline topologies near simple degenerate critical points in two-dimensional flow away from boundaries, Phys. Fluids 11 (1999) 314–324.
[13] D.D. Joseph, L. Sturges, The convergence of biorthogonal series for biharmonic and stokes flow edge problems: part II, SIAM J. Appl. Math. 34 (1978) 7–27.
[14] L.D. Sturges, Stokes flow in a two-dimensional cavity with moving end walls, Phys. Fluids 29 (1986) 1731–1734.
[15] P.H. Gaskell, M.D. Savage, J.L. Summers, H.M. Thompson, Stokes flow in closed rectangular domains, Appl. Math. Model. 22 (1998) 727–743.
[16] P.N. Shankar, M.D. Deshpande, Fluid mechanics in the driven cavity, Annu. Rev. Fluid Mech. 32 (2000) 93–136.
[17] F. Gürcan, Effect of the Reynolds number on streamline bifurcations in a double-lid-driven cavity with free surfaces, Comput. Fluids 32 (2003) 1283–1298.
[18] F. Gürcan, Streamline topologies near a stationay wall of Stokes flow in a cavity, Appl. Math. Comput. 165 (2005) 329–345.
[19] F. Gürcan, P.H. Gaskell, M.D. Savage, M.C.T. Wilson, Eddy genesis and transformation of Stokes flow in a double-lid driven cavity, Proc. Inst. Mech. Eng. Part C 217 (2003) 353–364.
[20] C.H. Driesen, J.G.M. Kuerten, M. Streng, Low-Reynolds-number flow over partially covered cavities, J. Engrg. Math. 34 (1998) 3–20.
[21] S.A. Trogdon, D.D. Joseph, Matched eigenfunction expansions for a slow flow over a slot, J. Non-Newton. Fluid Mech. 10 (1982) 185–213.
[22] J. Fadle, Die Selbstspannungs-Eigenwertfunktionen der quadratischen Scheibe, Ing. Arch. 11 (1941) 125–148.
[23] P.F. Papkovich, Über eine form der Lösung des Byharmonisschen Problems für das Rechtech, C. R. Dokl. Acad. Sci. URSS (NS) 27 (1970) 334–338.
[24] C.I. Robbins, R.C.T. Smith, A table of roots of $\sin z = -z$, Phil. Mag. 39 (1948) 1004–1005.